

Linking the dust and chemical evolution in Taurus and Perseus: new collisional rates for HCN, HNC, and their C, N, and H isotopologues.

Navarro-Almaida, D.¹, T. Bop, C.², Lique, F.², Esplugues, G.³,
Rodríguez-Baras, M.³, Kramer, C.⁴, E. Romero, C.⁵, Fuente, A.³, Caselli, P.⁶,
Riviére-Marichalar, P.³, and Mroczkowski, T.⁷

¹ Département d’Astrophysique (DAP), CEA, Orme des Merisiers, 91191 Gif sur Yvette, Paris-Saclay, France

² University Rennes, CNRS, Institut de Physique de Rennes (IPR) - UMR 6251, 35000 Rennes, France

³ Observatorio Astronómico Nacional (OAN), Alfonso XII, 3, 28014, Madrid, Spain

⁴ Institut de Radioastronomie Millimétrique (IRAM), 300 Rue de la Piscine, 38406 Saint Martin d’Hères, France

⁵ Center for Astrophysics, Harvard and Smithsonian, 60 Garden Street, Cambridge, MA 02143, USA

⁶ Centre for Astrochemical Studies, Max Planck Institute for Extraterrestrial Physics, Giessenbachstrasse 1, 85748 Garching, Germany

⁷ European Southern Observatory (ESO), Karl-Schwarzschild-Strasse 2, D-85741 Garching, Germany

Abstract

Despite their use as molecular probes and chemical clocks, the collisional rates of some of the C, N, and H isotopologues of HCN and HNC were, until now, absent. Here, we provide new collisional coefficients for these molecules and perform an up-to-date gas and dust chemical characterization of two different star-forming regions, TMC 1-C and NGC 1333-C7. With millimeter observations we derived their column densities, the C and N isotopic ratios, the isomeric ratios, and the deuterium fraction. Continuum data at 3 mm and 850 μm allowed us to compute the emissivity spectral index and look for grain growth, an evolutionary tracer. We found that gas temperature, deuterium fraction, and spectral index are complementary evolutionary tracers.

1 Introduction

The two isomers of the H-C-N system, hydrogen cyanide (HCN) and hydrogen isocyanide (HNC), are ubiquitous in the interstellar medium (ISM) and have been used to study its

physical and chemical properties [1, 2]. However, notorious cases show that the HCN/HNC chemistry is not fully understood yet (see, e.g., [3]).

Understanding isotopic abundance ratios is a major goal in modern astrochemistry. Rarer isotopologues are often used to determine physical conditions and as a proxy of the most abundant isotopologues as they do not usually suffer from opacity problems. A great limitation of this approach is the absence of collisional coefficients for the rarer isotopologues, forcing the assumption of isotopic ratios and leading to uncertainties [4]. The environment plays a crucial role in isotopic fractionation. Indeed, the abundance of molecules with deuterium is enhanced in the low-temperature gas prevailing in dense cores, becoming a diagnostic tool to determine the evolutionary stage of dense cores [5]. However, dating using deuterated molecules is limited by the absence of collisional rates for some of these species. Aiming to a better understanding of the chemistry and evolution of star-forming regions, we present collisional coefficients for the C, N, and H isotopologues of HCN and HNC.

Chemistry is not the only tool used to study the evolution of stellar objects, it can also be inferred by dust emission. In dense regions, grains are covered by icy mantles that make grains sticky, favoring grain coagulation, producing a different dust size distribution, and changing dust emissivity [6]. This change in dust emissivity is measured through the dust emissivity spectral index. In this work, we combine spectroscopic observations, dust continuum emission, and new collisional coefficients for the C, N, and H isotopologues of HCN and HNC to explore the chemical and physical evolution of the pre-stellar and protostellar envelopes during the first stages of the star formation process.

2 Collisional coefficients

Rate coefficients induced by collision with H_2 of the isotopologues of HCN and HNC, namely DCN, $D^{13}CN$, $H^{13}CN$, $HC^{15}N$, DNC, $DN^{13}C$, $HN^{13}C$ and $H^{15}NC$, are missing in the literature. Using the MOLSCAT computer code [7], we calculated state-to-state inelastic cross sections of these molecules induced by collision with p - H_2 . Variations of up to 50% in collisional rates have been found, having an impact of up to 30% in the brightness temperatures estimated using RADEX [8]. These new coefficients would therefore introduce an increase up to $\sim 30\%$ in the molecular hydrogen number density derived using these molecules.

3 Case study: TMC 1-C and NGC 1333

In this section we assess the impact of these new collisional coefficients in astrochemical modeling. We used the emission spectra of the $J = 1 \rightarrow 0$ rotational transitions of HCN, HNC, and their ^{13}C , ^{15}N , and D isotopologues towards positions in TMC 1-C and NGC 1333-C7 (Figure 1 and Table 1), observed with the Yebes 40m telescope.

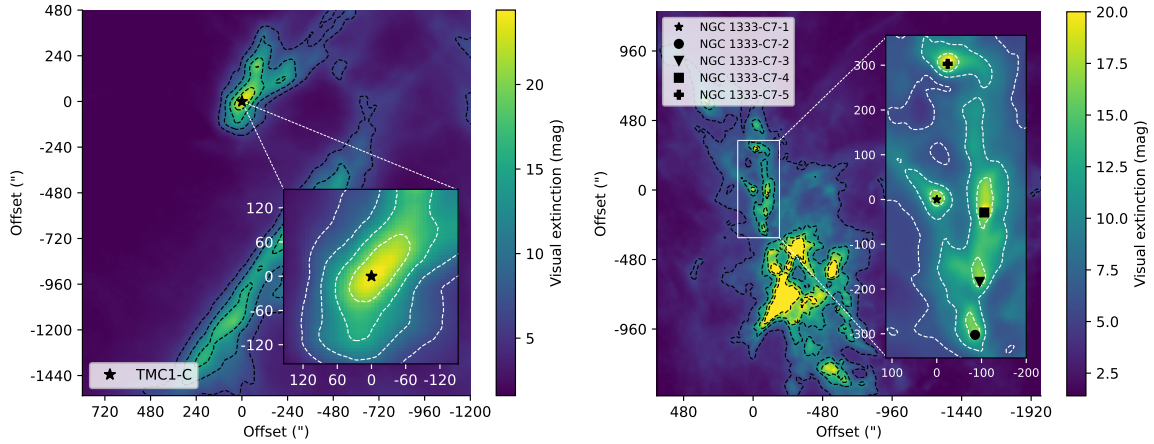


Figure 1: Visual extinction map of TMC 1-C (left) and NGC 1333-C7 (right)

Table 1: Target positions, spectral classes, and radii.

Source	RA (2000)	Dec (2000)	Class
TMC 1-C	04:41:37.58	26:00:31.10	Starless core
NGC 1333-C7-1	03:29:25.57	31:28:14.83	Class 0
NGC 1333-C7-2	03:29:19.05	31:23:14.45	Class I
NGC 1333-C7-3	03:29:18.29	31:25:08.34	Starless core ¹
NGC 1333-C7-4	03:29:17.38	31:27:46.09	Class 0
NGC 1333-C7-5	03:29:23.95	31:33:18.15	Class 0

3.1 Molecular column densities

From the line emission we derived the column densities of the species using the new collisional coefficients and the RADEX [8] radiative transfer code. In all positions belonging to NGC 1333-C7, the gas temperature is assumed to be ~ 15 K, similar to the dust temperature derived from the *Herschel* space telescope maps of [9]. For TMC 1-C, we adopted $T_{\text{kin}} = 8$ K following the calculations of [10, 5]. The density was assumed to be $n_{\text{H}} = 4 \times 10^5 \text{ cm}^{-3}$, a reasonable value for our sample [5, 11]. Our collisional rates do not consider hyperfine splitting, so in the case this splitting is present, the column density was obtained reproducing the integrated flux of the weakest hyperfine component observed. Then, the total column density is scaled using the relative intensities of the hyperfine components from the CDMS catalogue.

¹NGC1333-C7-3 class is uncertain as it was classified as starless core by default since it did not fit the criteria of any other class.

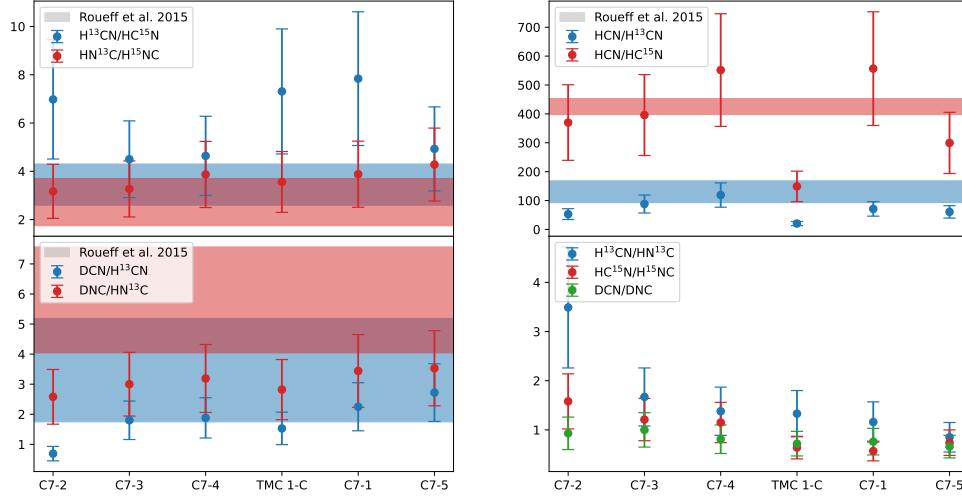


Figure 2: Blue, red, and green dots represent the different observed molecular ratios across the positions analyzed in this paper. The horizontal bands span from the minimum to the maximum values for the ratios obtained in the models of [4]. The sources are ordered by decreasing dust temperature.

3.2 Isotopic and isomeric ratios

Figure 2 shows the resulting column density ratios. We found a differentiated behavior between the two isomers. The isotopic ratios involving HNC, the $\text{HN}^{13}\text{C}/\text{H}^{15}\text{NC}$ and $\text{DNC}/\text{HN}^{13}\text{C}$ present uniform values across the sample. However, we detected variations in those of HCN, in particular $\text{DCN}/\text{H}^{13}\text{CN}$, $\text{H}^{13}\text{CN}/\text{HN}^{13}\text{C}$, and $\text{HC}^{15}\text{N}/\text{H}^{15}\text{NC}$ ratios show systematic changes with core evolution. The $\text{H}^{13}\text{CN}/\text{HN}^{13}\text{C}$ ratio we computed across our sample shows a trend that can be interpreted as a progressive increase in the average gas temperature from the coldest core starless cores NGC1333-C7-5 and TMC 1-C to the Class I source NGC1333-C7-2 [2]. This interpretation is consistent with the decreasing deuterium fraction $\text{DCN}/\text{H}^{13}\text{CN}$, as deuteration in the gas phase is less efficient in warmer gas. The $\text{H}^{13}\text{CN}/\text{HN}^{13}\text{C}$ ratio therefore becomes an evolutionary tracer of our sample, from the colder, less evolved members, to the warmer and more evolved members.

3.3 Continuum emission, grain growth, and evolution

The freeze out of molecules during the evolution of prestellar cores and ice growth are linked to grain coagulation, changing the emission properties of the grains, measured by the dust emissivity spectral index β . Here we examine the behavior of β using 3 mm MUSTANG-2 images and Herschel data at 850 μm . Assuming a modified blackbody model:

$$\beta_{0.85\text{mm}-3\text{mm}} = \frac{\log(\tau_{3\text{mm}}/\tau_{0.85\text{mm}})}{\log(\nu_{3\text{mm}}/\nu_{0.85\text{mm}})}, \quad I_\nu = B_\nu(T_d)\tau_\nu, \quad (1)$$

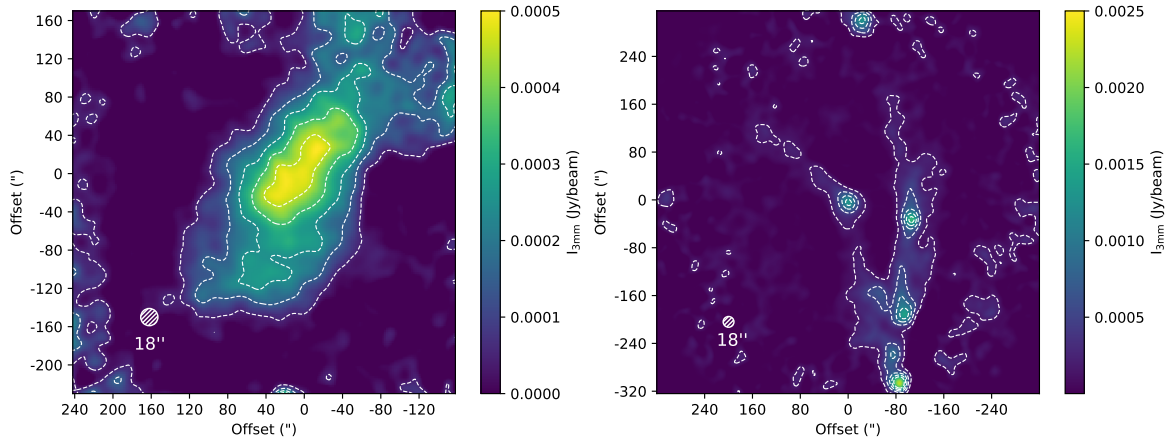


Figure 3: *Left panel:* Flux at 3 mm in the TMC 1-C prestellar core. *Right panel:* Flux at 3 mm in the NGC 1333-C7 sector.

and combining the information of the extinction maps in Figure 1, the dust temperature data [9], and the 3 mm continuum flux maps in Figure 3, we obtain the dust optical depth at 850 μm and 3 mm, and the dust emissivity spectral index $\beta_{0.85\text{mm}-3\text{mm}}$ (see Table 2). Our results show that the Class I object NGC1333-C7-2 presents the lower spectral index, $\beta_{0.85\text{mm}-3\text{mm}} \sim 1.1 - 1.3$, consistent with the presence of large grains in its protostellar disk. The spectral index of the Class 0 members of the sample is found to be higher, in the range 1.6 – 1.7 and, finally, of around ~ 2 for the prestellar core TMC 1-C. We conclude that the value of β at millimeter wavelengths is useful to discern starless cores and Class 0 objects from Class I protostars, pointing to the existence of grain growth in the Class I protostellar disks. This is coherent with the chemical information obtained from the HCN and HNC molecules about temperature and deuterium fraction, as more evolved sources are warmer, exhibit less deuterium fractionation, and show lower spectral indexes, a sign of grain growth (Figure 4).

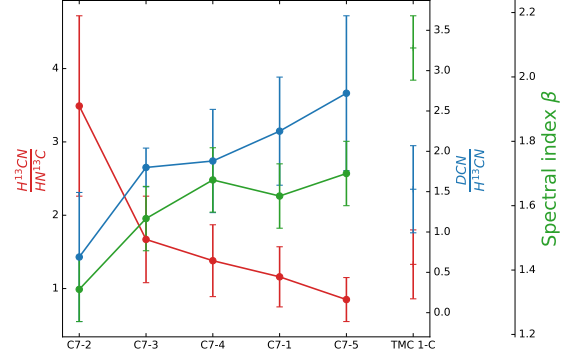
4 Summary and conclusions

We performed a chemical study of two different star-forming regions with updated collisional rates to investigate their chemical and evolutionary characteristics:

- We presented new collisional coefficients of HCN, HNC, and their C, N, and H isotopologues. We computed the $^{13}\text{C}/^{12}\text{C}$ and $^{15}\text{N}/^{14}\text{N}$ isotopic ratios, deuterium fractions, and isomeric ratios, showing good agreement with current chemical models [4]. The ratios between the two isomers show different variability across our sample, suggesting a different origin of their emission. The $\text{H}^{13}\text{CN}/\text{HN}^{13}\text{C}$ ratio is found to be a proxy of the temperature. The deuterium fraction of HCN is an evolutionary tracer past the prestellar phase since it decreases as heating from the nascent star increases the gas and dust temperature.

Table 2: Continuum 3 mm flux, optical depth at 850 μm and 3 mm, and the spectral index.

Position	$\tau_{3\text{mm}} \times 10^4$ (18")	$\tau_{850\mu\text{m}} \times 10^3$ (18")	$\beta_{0.85\text{mm}-3\text{mm}}$ (18")
TMC 1-C	0.82 ± 0.02	1.43 ± 0.14	2.09 ± 0.08
NGC1333-C7-1	1.35 ± 0.04	1.26 ± 0.13	1.63 ± 0.09
NGC1333-C7-2	1.85 ± 0.03	1.15 ± 0.12	1.34 ± 0.08
NGC1333-C7-3	1.26 ± 0.04	1.09 ± 0.11	1.56 ± 0.09
NGC1333-C7-4	1.65 ± 0.04	1.64 ± 0.16	1.68 ± 0.09
NGC1333-C7-5	1.54 ± 0.05	1.57 ± 0.16	1.70 ± 0.09

Figure 4: Values of the $\text{H}^{13}\text{CN}/\text{HN}^{13}\text{C}$ (red) and $\text{DCN}/\text{H}^{13}\text{CN}$ (blue) ratios, and the spectral index (green) across the sources of our sample.

- We analyzed the continuum emission of our sample to estimate the spectral index. The dust spectral index is found to be $\beta_{0.85\text{mm}-3\text{mm}} = 1.34$ for the most evolved member of our sample, and rises up to $\beta_{0.85\text{mm}-3\text{mm}} = 2.09$ in TMC 1-C, a prestellar core. We find a tentative correlation between the spectral index and the HCN deuterium fraction. This is consistent with the presence of grain growth in evolved objects past the prestellar phase as the dust and gas temperatures increase, thus reducing the HCN deuterium fraction.

References

- [1] Aalto, S., Garcia-Burillo, S., Muller, S., et al. 2012, A&A, 537, A44
- [2] Hacar, A., Bosman, A. D., & van Dishoeck, E. F. 2020, A&A, 635, A4
- [3] Hily-Blant, P., Walmsley, M., Pineau Des Forêts, G., & Flower, D. 2010, A&A, 513, A41
- [4] Roueff, E., Loison, J. C., & Hickson, K.M. 2015, A&A, 576, A99
- [5] Navarro-Almaida, D., Fuente, A., Majumdar, L., et al. 2021, A&A, 653, A15
- [6] Ormel, C. W., Paszun, D., Dominik, C., & Tielens, A. G. G. M. 2009, A&A, 502, 845
- [7] Hutson, J. & Green, S. 1994, Collaborative computational project
- [8] van der Tak, F. F. S., Black, J. H., Schöier, F. L., Jansen, D. J., & van Dishoeck, E. F. 2007, A&A, 468, 627
- [9] Zari, E., Lombardi, M., Alves, J., Lada, C. J., & Bouy, H. 2016, A&A, 587, A106
- [10] Navarro-Almaida, D., Le Gal, R., Fuente, A., et al. 2020, A&A, 637, A39
- [11] Rodríguez-Baras, M., Fuente, A., Rivière-Marichalar, P., et al. 2021, A&A, 648, A120
- [12] Milam, S.N., Savage, C., Brewster, M.A., Ziurys, L.M., & Wyckoff, S. 2005, ApJ, 634, 1126
- [13] Colzi, L., Sipilä, O., Roueff, E., et al. 2013, A&A, 560, A3
- [14] Caselli, P., Walmsley, C. M., Tafalla, M., Dore, L., & Myers, P. C. 1999, ApJ, 523, L165
- [15] Tafalla, M., Santiago-García, J., Myers, P. C., et al. 2006, A&A, 455, 577